


Cite this: *RSC Adv.*, 2020, 10, 9341

Received 17th December 2019
Accepted 17th February 2020

DOI: 10.1039/c9ra10624c

rsc.li/rsc-advances

An electroless-plating-like solution approach for the preparation of PS@TiO₂@Ag core-shell spheres

Chao Wang,^{†a} Daichuan Ma,^{†b} Xinsheng Li,^c Daibing Luo^{ID}*^b and Liangzhan Wu*^d

PS@TiO₂@Ag spheres with triple-level core-shell nanostructures were prepared *via* a versatile coating procedure based on an electroless-plating-like solution deposition (EPLSD) method. A peroxo-titanium-complex (PTC) aqueous solution was used as the precursor to react with an aniline monomer in the EPLSD preparation. Aniline plays an important role in the TiO₂ layer anchoring process through the swollen effects of the PS cores. As extended, peroxo-metal-complex (PMC) with the d⁰ configuration can be introduced onto PS spheres to form varieties of PS@metal oxide core-shell structures by this method under mild conditions. Ag layers were then modified onto the PS@TiO₂ spheres *via* the photocatalytic method. By the extraction of the PS cores, hollow TiO₂ and TiO₂@Ag spheres could be obtained. The photochemical degradation of methylene blue (MB) under UV light irradiation was performed on the composite nanostructures.

1. Introduction

Core-shell nanostructures are effective sources for the construction of many numerous advanced materials.^{1,2} Most of the shell materials can be substituted by inexpensive core species to reduce the consumption of the expensive shell materials. Among the core-shell nanostructures, titania (TiO₂)-polystyrene (PS) composites are good templates to generate inorganic-coated polymer encapsulation, hollow spheres, or composite nanomaterials.^{3–5} Titania is very attractive owing to its high chemical and thermal stability, and excellent electronic and optical properties.^{6,7} The construction of TiO₂ with core-shell structures is a promising strategy to tune its properties without its obvious side effects. Moreover, PS substrates can be easily prepared with narrow size distribution over a wide size range, which is an ideal substrate for TiO₂ loading. A large number of synthetic strategies for core-shell materials based on TiO₂-PS have been developed, which are mainly divided into two categories: top-down^{8,9} and bottom-up methods.^{10,11} Among these, the sol-gel method is highly versatile and does not require complicated operations and expensive instruments. Based on this method, great efforts have been made to develop

titania shell coating procedures using aqueous solution media.^{12,13}

However, the uniform deposition of crystalline TiO₂ as thin layer shells in core-shell structures *via* a simple one-pot procedure is still a big challenge, which may be due to the low electronic negativity and high coordination numbers of titanium. Therefore, it is difficult to control the reaction kinetics of the heterogeneous nucleation for the shell TiO₂ growth on the cores since the condensation and hydrolysis of titania precursors are rapid to control the coating processes *via* a sol-gel method.¹¹ In this case, inhibitor agents are often used to slow down the rate of the condensation and hydrolysis of titania precursors.¹⁴ In addition, crystalline metal oxides (*e.g.*, TiO₂) formed by sol-gel routes typically require annealing steps at high temperatures, which may result in the destruction of the formed core-shell structures.

In practical applications, TiO₂ suffers from poor visibility and IR absorption due to the large band gap (~3.0 eV), which limits its efficiency for photocatalysis and energy conversion. The doping of metal species may modify the photochemical properties of TiO₂. Hence, combining the TiO₂-PS core-shell nanostructures with modified metals may generate new types of composites with enhanced photochemical activity, which can be used in photocatalysis, photothermal therapy, energy storage, or solar energy conversion. More importantly, metal or metal oxide-assisted TiO₂ photocatalytic degradation is considered as an efficient method for the removal of organic wastes.¹⁵ This type of photocatalyst with hollow or porous structures can lower the diffusion resistance of reactants, thus boosting their diffusion as well as trapping the incident light for a long time to achieve high efficiency for photon utilization.

^aCollege of Chemistry, Sichuan University, No. 29, Wangjiang Road, Wuhou District, Chengdu, 610064, P. R. China

^bAnalytical & Testing Center, Sichuan University, No. 29, Wangjiang Road, Wuhou District, Chengdu, 610064, P. R. China. E-mail: luodb@scu.edu.cn

^cCollege of Computer Science, Sichuan University, No. 29, Wangjiang Road, Wuhou District, Chengdu, 610064, P. R. China

^dTechnical Institute of Physics and Chemistry, Chinese Academy of Sciences, Beijing, 100190, P. R. China. E-mail: wuliangzhan@mail.ipc.ac.cn

[†] The authors contributed equally to this work.

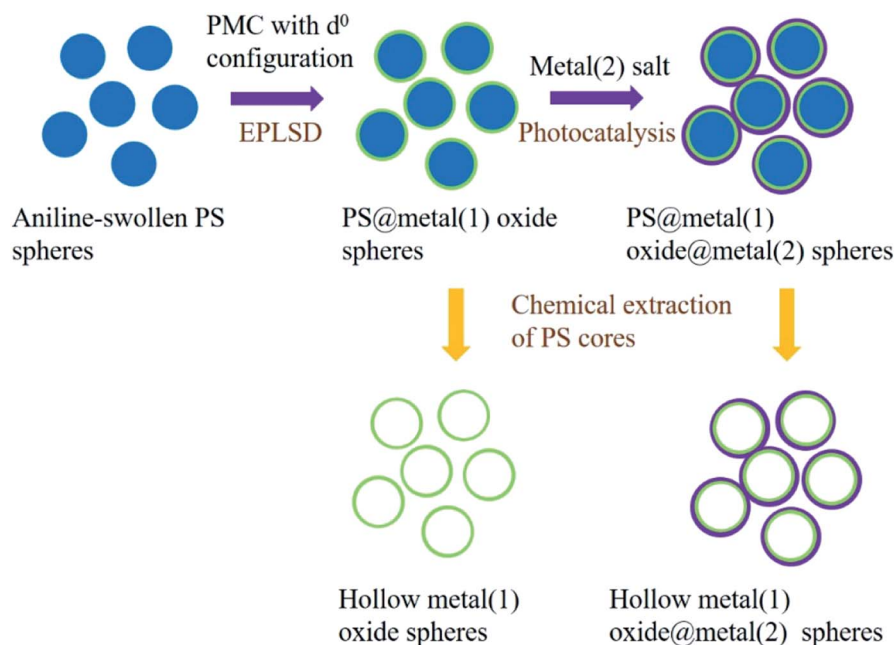

Herein, we have developed a versatile method to synthesize monodispersed PS@TiO₂@Ag core-shell structures using the electroless-plating-like solution deposition (EPLSD) strategy, as shown in Scheme 1.^{16,17} Electroless plating is a non-galvanic method for simultaneous redox reactions between metal ions in aqueous solutions to form metal films at room temperature. In this preparation, PS cores are swollen-treated by aniline for the further modification of TiO₂ shells. It is a novel strategy to prepare multi-level core-shell nanostructures where the *in situ* crystallization of oxides occurs at low temperatures. For example, other types of peroxo-metal-complex precursors using metal oxides with d⁰ configurations, such as peroxo-molybdenum-complex (PMC) or peroxo-vanadium-complex (PVC) can be used to replace peroxo-titanium-complex (PTC), forming the PS@MoO₃@Ag or PS@V₂O₅@Ag nanocomposite structures. Moreover, the anchored Ag nanoparticles onto the metal oxide layer may also replace other metal shells by using other metal salt solutions, such as HAuCl₄ or Cu(NO₃)₂ to form Au- or Cu-modified layers. In addition, hollow metal oxide spheres or metal(1) oxide@metal(2) spheres can further be obtained by the chemical extraction of the PS cores. The unique nanostructure can increase the surface area and provide more active sites for better electrolyte infiltration. Moreover, the void space in hollow nanostructures can serve as soft mediums for the adsorption of ions and shorten the ion transportation route.¹⁸ This method towards preparing multi-level PS@metal(1) oxide@metal(2) nanocomposites provides an alternative for the titania-based core-shell nanostructures, which is highly different from the Stöber-related coating procedure. In comparison with our previous studies, it is the first time that we construct the multi-layer structures *via* a one-pot procedure by the EPLSD method, where the *in situ* crystallization of metal oxides occurs at a low temperature.

2. Experimental

The synthesis procedure is illustrated in Scheme 1. First, PS spheres were prepared by a polymerization method *via* emulsifier-free emulsion. 180 mL of water and 9 g of styrene were added into a four-necked round flask (250 mL) and heated up to 70 °C. Before introducing the initiator, the mixture solution was purged with nitrogen to eliminate the inhibiting effects of oxygen, and then AIBA (2,2'-azobis[2-methylpropionamidine] dihydrochloride) dissolved in pure water (0.18 g 15 mL⁻¹) was added into the solution. The polymerization was performed under nitrogen atmosphere protection with mechanical stirring for 24 h before cooling to room temperature, and the PS spheres were obtained.

Moreover, the peroxo-titanium-complex (PTC) precursor solution was prepared through TiCl₄ which in turn was treated with ammonia to form titanic acid precipitates. The precipitate was dissolved in 30 wt% H₂O₂ solution, followed by diluting to M [Ti] = 0.125 mol L⁻¹ to prepare the PTC precursor solution. Similarly, other peroxo-metal-complex (PMC, with d⁰-configured metals) precursor solutions can be prepared similar to the PTC precursor solution.

The PS@TiO₂ nanostructures were prepared *via* the anchoring of the PTC precursor onto the aniline swollen-treated PS spheres. Aniline was added into water (15 mL) at 0 °C through an ultrasonic treatment for 15 min, followed by the introduction of the as-prepared PS (1.2 g). The mixture was stirred for 30 min at 0 °C to anchor aniline molecules onto the PS seed surface through a swelling process. Then, the dispersion of the PS particles swollen with aniline was transferred into a three-necked round bottom flask placed in an ice bath, and the PTC aqueous solution was then added into the dispersion



Scheme 1 Illustration of the preparation of PS@metal(1) oxide@metal(2) nanocomposites with core-shell structures, and their relative hollow spheres.



with a PTC/aniline molar ratio of a 2 : 1. Then, the TiO₂ shell was formed on the PS core surface at 80 °C *via* the EPLSD process for 30 min. Similarly, other types of metal (with the d⁰ configuration) oxide shells *via* the EPLSD process can be obtained with their corresponding precursors (PMC). Finally, Ag nanocrystals (NCs) were modified onto the PS@TiO₂ spheres using the AgNO₃ solution by a UV photocatalytic (254 nm ultraviolet irradiation) method to form the PS@TiO₂@Ag core-shell nanostructures.

The surface morphologies of the samples were examined *via* field-emission scanning electron microscopy (FE-SEM, JSM-7500F, JEOL, Japan). X-ray diffraction (XRD) experiments were performed using an XD-2 diffractometer (Purkinje General Instrument Co. Ltd.) with Cu K α radiation at 36 kV and 30 mA. The transmission electron microscopy (TEM, Tecnai G2 F20, FEI, USA) was performed at an operating voltage at 100 kV to observe the microstructure of the samples. Energy dispersive X-ray spectroscopy (EDS) analysis was performed to characterize the element type and content.

The photocatalytic performance towards the methylene blue (MB) degradation was performed under UV irradiation (365 nm) in an aqueous solution (20 mg mL⁻¹, 50 mL) using the composites as the photocatalysts (0.1 mg mL⁻¹). The suspension was magnetically stirred at room temperature. At last, 3 mL of the solution was taken out as the sample. After centrifugation to remove the solid residues, the sample was analyzed *via* UV-vis spectroscopy. After each degradation experiment, the nanocomposites were separated and soaked in HCl solution (1 M, 50 mL) for 1 h, rinsed and dried under UV irradiation, and then were reused for the next test.

3. Results and discussion

3.1. PTC effect

It is difficult for the TiO₂ shells to grow on bare PS substrate without proper pretreatments.^{19,20} In this preparation, PTC with d⁰-configured titanium is employed as the titania precursor instead of the widely used tetrabutyltitanate (TBOT).¹⁵ Another difference from other preparations is the use of aniline to swell the PS spheres. By controlling the redox reaction between the PTC precursor and aniline that is swollen into PS cores, preferential heterogeneous nucleation and growth of crystalline TiO₂ shells on the core surface can be easily realized without an additional calcination process.²¹ The role of aniline on surface modification is very important in the preparation process.

The nanosized charge-stabilized PS seed latex was readily formed in the emulsifier-free emulsion polymerization and could be further used without any post-treatment. Upon mixing the yellow oil droplets of aniline with the as-prepared PS cores, the added aniline monomer was distributed between the organic species and aqueous phase. Aniline is an ideal solvent for PS, but its aqueous solubility is limited. Therefore, aniline molecules are absorbed into the PS beads after a certain period of stirring with ultrasonic assistance, forming aniline-swollen PS particles that are highly dispersed. As shown in Fig. 1(a), the as-prepared PS cores have a diameter of around 380 nm. After the treatment of the PS spheres with aniline, the PTC

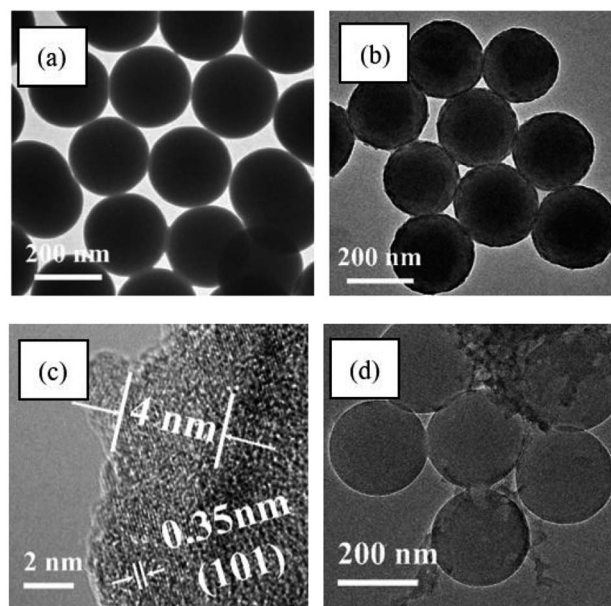


Fig. 1 TEM images of (a) PS cores, (b) PS@TiO₂ spheres prepared by PTC coating on aniline swollen PS cores, (c) HRTEM analysis on the PS@TiO₂ particle surface, (d) effect of PTC coating on untreated PS cores.

solution was subsequently added into the solution of aniline-swollen PS spheres at 80 °C for 30 min through the EPLSD procedure, forming the PS@TiO₂ core-shell nanostructure. As shown in Fig. 1(b), the as-prepared PS@TiO₂ composite spheres have the same spherical shape but rougher surface in comparison with the PS seed spheres. High-resolution TEM (HRTEM) image (Fig. 1(c)) reveals that a well-crystallized TiO₂ shell with a 4 nm thickness was formed on the sphere surface. The (101) facet of anatase TiO₂ with a 0.35 nm spacing was identified. As shown in Fig. 1(d), only a small amount of TiO₂ nanoparticles obtained through the heterogeneous nucleation growth are randomly distributed on the untreated PS spherical surface instead of the aniline-swollen PS in the EPLSD process, revealing that the aniline treatment is a key factor in the EPLSD preparation. As reported in our previous study, the EPLSD procedure is highly dependent on a redox reaction between PTC and aniline, in which PTC is reduced to TiO₂, and the aniline is polymerized to polyaniline as oxide. Therefore, the TiO₂-shell coating can be formed on aniline-swollen PS spheres *via* the EPLSD process, while bare PS species can hardly anchor the TiO₂ nanoparticles obtained *via* the decomposition of PTC precursors.

3.2. SEM and XRD characterizations

In our previous studies, by using the EPLSD method, flexible films modified by metal oxides were successfully fabricated,^{17,21} and polyaniline/titania nanocomposites with porous networks were obtained.¹⁶ In this study, we extended the EPLSD method to construct multi-layer spheres with different types of materials. Through SEM observation, the obtained PS spheres have a narrow size distribution, as shown in Fig. 2(a). Their average

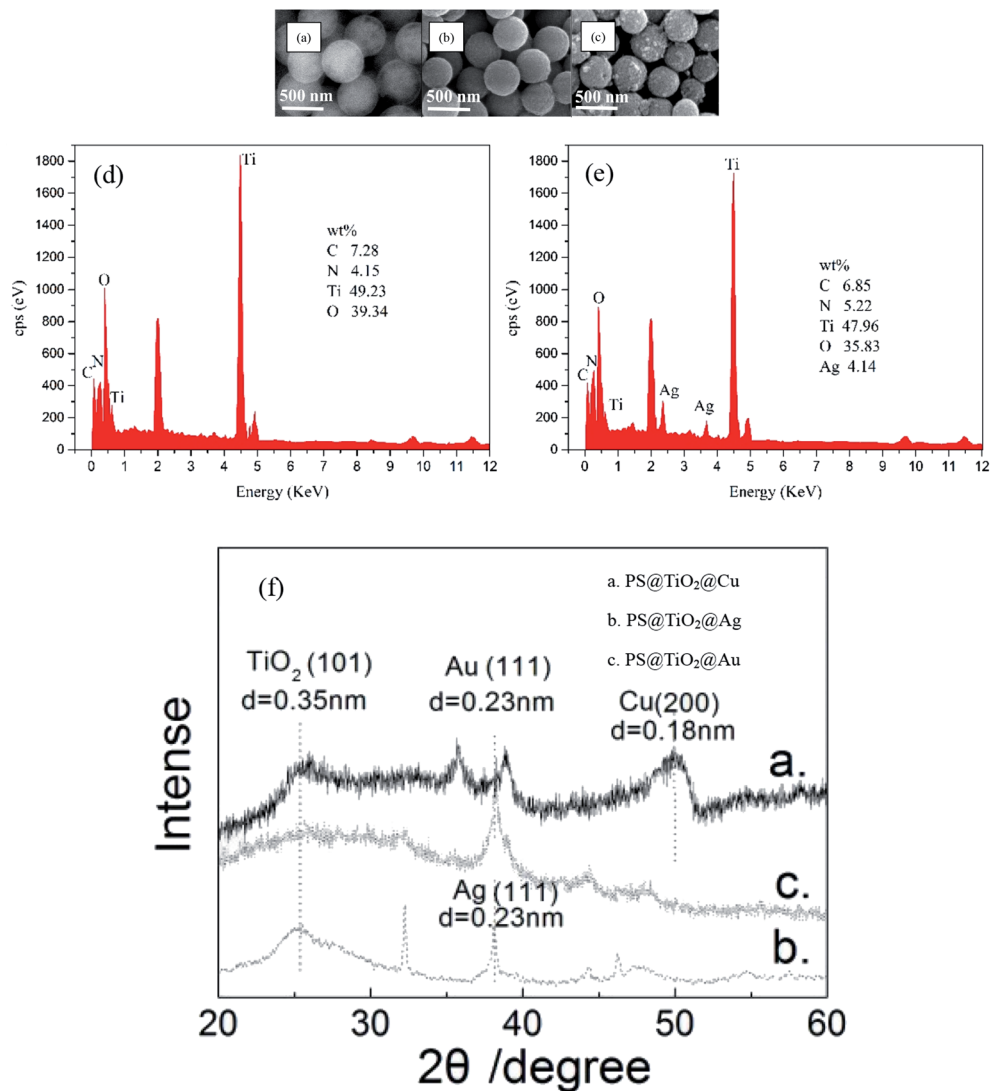


Fig. 2 SEM images of (a) PS spheres, (b) PS@TiO₂ spheres, (c) PS@TiO₂@Ag spheres; and EDS of (d) PS@TiO₂ spheres, (e) PS@TiO₂@Ag spheres; and (f) XRD patterns of PS@TiO₂@metal (Au, Ag, Cu) nanocomposites.

diameter is about 380 nm. After covering with TiO₂ layers, the sphere surface turned from smooth to rough, as compared in Fig. 2(a) and (b). The *in situ* UV photocatalytic deposition of Ag nanoparticles on the titania layer to generate the PS@TiO₂@Ag nanostructure is based on the charge transfer (CT) from TiO₂ to the adsorbed metal particles.^{22,23} After the further deposition of Ag layers onto the PS@TiO₂ surface, a rather rough surface on the Ag-modified spheres is observed (Fig. 2(c)), which may be caused by a different photocatalytic redox efficiency on different anatase facets.^{24,25} The element analysis revealed the presence of C, N, O, and Ti elements in the PS@TiO₂ (Fig. 2(d)), and the presence of C, N, O, Ti, and Ag elements in the PS@TiO₂@Ag (Fig. 2(d)) material, which confirms that the shell species are successfully uploaded onto the previous cores. The chemical components in the core-shell nanostructures were further characterized *via* X-ray diffraction (XRD), as shown in Fig. 2(f), which confirms the presence of anatase TiO₂ formed in the crystalline phase (JCPDS: 02-0406). In addition, three types of

PS@TiO₂@metal (Au, Ag, and Cu) nanocomposites prepared by the EPLSD method were measured for comparison. The diffraction peaks are identified as TiO₂ (101) 25.5°, Ag (111) 38.1°, Au (111) 38.3°, and Cu (200) 50.1°, respectively.

3.3. TiO₂ layer effect

It is well known that the charge transfer (CT) from TiO₂ to the adsorbed molecules can be used for the photocatalytic deposition of metal nanocrystals (NCs) on titania.²⁶ Fig. 3(a) indicates that the sphere surface was successfully decorated with Ag NCs. The PS@TiO₂@Ag core-shell spheres have a slightly rough surface, as shown in Fig. 3(b), which is different from that of the PS@TiO₂ spheres. The HRTEM image (Fig. 3(c)) on the sphere surface shows the crystalline structure and the distance between two adjacent lattice planes is about 0.23 nm, which is in agreement with the lattice spacing of the Ag (111) facets. The average thickness of the Ag layers is estimated to about 4 nm. As



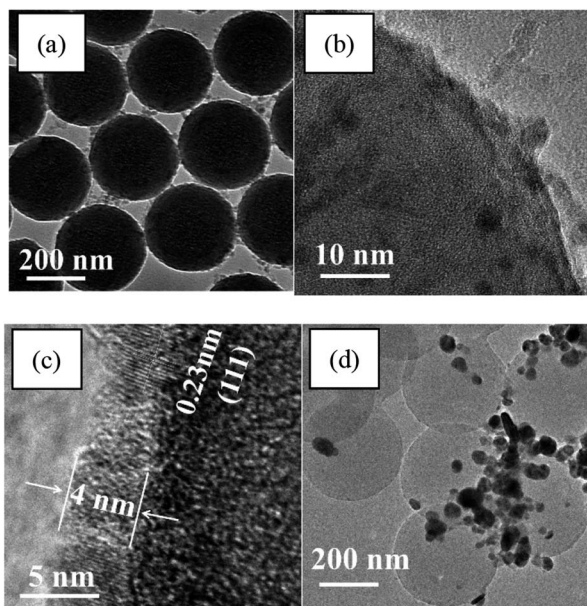


Fig. 3 TEM images of (a) PS@TiO₂@Ag spheres, (b) magnified TEM image of an individual PS@TiO₂@Ag sphere at the surface, (c) HRTEM image for the surface layer analysis, (d) TEM image of the effects of the photocatalytic deposition of Ag NCs on PS spheres without TiO₂ layers.

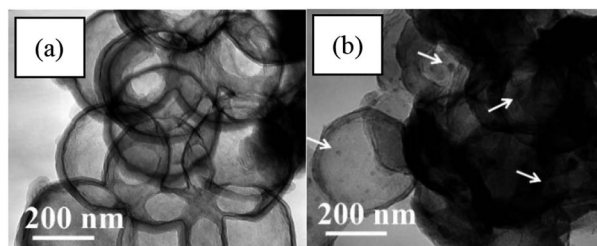


Fig. 4 (a) Remaining TiO₂ and (b) TiO₂@Ag residue spheres after the tetrahydrofuran extraction of the PS cores from the composite spheres.

compared, if only the PS spheres are used as the cores without TiO₂ layers, only a few Ag nanoparticles (NPs) are separately absorbed onto the PS surface (Fig. 3(d)) in the photocatalytic deposition process, indicating that the TiO₂ intermediate layer plays an important role in the metal layer modification.

3.4. Hollow spheres

Hollow structures provide high cycling performance, specific active area, and superior rate capability.²⁷ The PS core extraction was performed to obtain hollow TiO₂ and hollow TiO₂@Ag nanostructures. TEM images which are shown in Fig. 4(a) and (b) demonstrate the TiO₂ and TiO₂@Ag residues as hollow spheres after immersing the PS@TiO₂ and PS@TiO₂@Ag spheres in tetrahydrofuran overnight, respectively. After the extraction treatment, the remained shells are clearly seen. Some Ag NCs with larger size are clearly seen on the surface of the hollow TiO₂@Ag spheres (indicated by the arrows in Fig. 4(b)). The average size of the Ag NCs is about 2–4 nm evaluated from the observation.

3.5. Degradation test

The multi-layer phase of this kind of nanocomposite is a highly desirable structure for high-performance photocatalysis. MB in an aqueous solution was used as a model target to test the photocatalytic activity of the nanocomposites, and the results are compared in Fig. 5(a). It was found that about 86.1% and 88.2% of MB could be degraded after 120 min on the hollow TiO₂@Ag and PS@TiO₂@Ag spheres, respectively, suggesting a better photocatalytic property of the core-shell nanostructure due to the synergic effects of TiO₂ and Ag shells. Ag NCs compacted with the TiO₂ layers could enhance their practical potential in harsh environments. It is considered that Ag NCs confined in a core-shell hollow TiO₂ photocatalyst may exhibit photocatalytic activity under solar light irradiation.¹⁵ In addition, the multiple light reflection and scattering from the mixing phases of Ag and TiO₂ are other crucial factors of the photocatalytic activity.^{28,29} The influence of Ag in the nanocomposites on the photocatalytic degradation was also evaluated. As shown in Fig. 5(a), the photoactivity of the PS@TiO₂

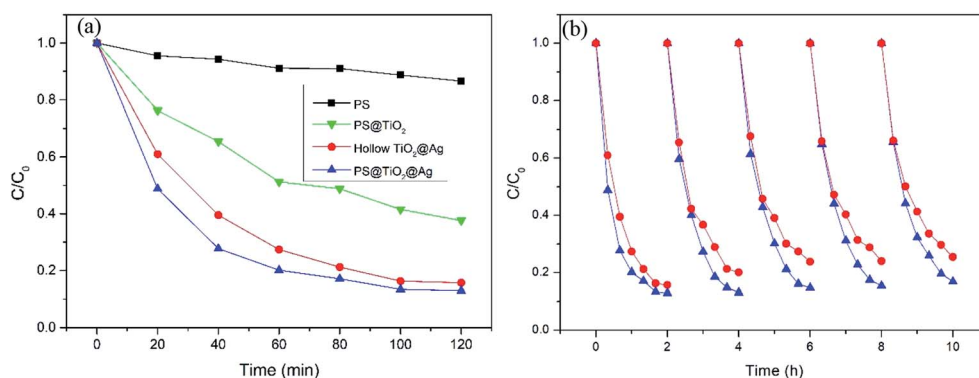


Fig. 5 (a) Photocatalytic degradation of MB in an aqueous solution under UV light (365 nm) on PS spheres, PS@TiO₂ spheres, PS@TiO₂@Ag nanocomposites, and hollow TiO₂@Ag spheres; (b) cycling test for MB degradation on hollow TiO₂@Ag and PS@TiO₂@Ag nanocomposites (blue triangle: PS@TiO₂@Ag, red circle: hollow TiO₂@Ag).



sphere alone is not ideal in comparison with that of Ag-modified ones. Moreover, the stability of the composites was examined in the degradation for five repeated cycles, and the results indicated favorable stability of this core-shell nanostructure (Fig. 5(b)). In comparison with the TiO₂ single shell, this kind of composite photocatalyst can use the anchored Ag layer as the electron transfer channel and reservoir, thus improving the lifetime of the photogenerated charge pairs. Further progress on this kind of hollow spheres is currently under investigation for optimally photocatalytic applications.

4. Conclusions

A facile method to prepare PS@TiO₂@Ag core-shell nanostructures using an EPLSD strategy has been developed. By the careful regulation of the redox reaction between the PTC precursors and aniline, the heterogeneous nucleation and growth of crystalline TiO₂ shells on the PS cores could be achieved under mild conditions. Other types of metal oxide shells for core-shell nanostructures *via* the EPLSD process could be obtained with their corresponding PMC precursors. Furthermore, PS@metal(1) oxide@metal(2) composite spheres could be alternatively obtained *via* the photocatalytic deposition of metal(2) NC layers onto PS@metal(1) oxide previously prepared by PMC precursors and PS cores based on the CT mechanism. Moreover, hollow TiO₂ or TiO₂@Ag nanocomposite spheres were obtained by the chemical extraction of the PS cores. The photocatalytic degradation of MB by the PS@TiO₂@Ag spheres and hollow TiO₂@Ag demonstrates the desirable photoactivity of the nanostructures. Our study overcomes the disadvantages of numerous TiO₂-based photocatalysts for unideal degradation efficiency.

Conflicts of interest

The authors declare no competing financial interest.

Acknowledgements

We acknowledge the Basic Research Funding for Breeding Project of Sichuan University (2019-21), the Fundamental Research Funds for the Central Universities (20826041C4202), and the funding from Science & Technology Department of Sichuan Province (2017JY0270). We thank Engineer Yi He's operation on the SEM imaging and Dr Jiqiu Wen's help of XRD measurements from Analytical & Testing Center of Sichuan University.

Notes and references

- O. D. Velev, T. A. Jede, R. F. Lobo and A. M. Lenhoff, *Nature*, 1997, **389**, 447–448.
- H. Y. Hu, Y. Lin and Y. H. Hu, *Chem. Eng. J.*, 2019, **375**, 122029.

- J. Shao, W. C. Sheng, M. S. Wang, S. J. Li, J. R. Chen, Y. Zhang and S. S. Cao, *Appl. Catal., B*, 2017, **209**, 311–319.
- J. Q. Zhang and L. Zhang, *ACS Appl. Nano Mater.*, 2019, **2**, 6368–6377.
- F. Z. Shi, Y. G. Li, H. Z. Wang and Q. H. Zhang, *Appl. Catal., B*, 2012, **123–124**, 127–133.
- X. B. Chen and S. S. Mao, *Chem. Rev.*, 2007, **107**, 2891–2959.
- D. B. Luo, B. S. Liu, A. Fujishima and K. Nakata, *ACS Appl. Nano Mater.*, 2019, **2**, 3943–3950.
- H. Li, R. M. Vilar and Y. M. Wang, *J. Mater. Sci.*, 1997, **32**, 5545–5550.
- A. C. Dodd, *Powder Technol.*, 2009, **196**, 30–35.
- R. G. Chaudhuri and S. Paria, *Chem. Rev.*, 2012, **112**, 2373–2433.
- Y. Bao, Q. L. Kang, C. Liu and J. Z. Ma, *Mater. Lett.*, 2018, **214**, 272–275.
- W. Li, J. P. Yang, Z. X. Wu, J. X. Wang, B. Li, S. S. Feng, Y. H. Deng, F. Zhang and D. Y. Zhao, *J. Am. Chem. Soc.*, 2012, **134**, 11864–11867.
- J. S. Chen, C. P. Chen, J. Liu, R. Xu, S. Z. Qiao and X. W. Lou, *Chem. Commun.*, 2011, **47**, 2631–2633.
- Z. L. He, W. X. Que and Y. C. He, *Mater. Lett.*, 2013, **94**, 136–139.
- S. D. Zhao, J. R. Chen, Y. F. Liu, Y. Jiang, C. G. Jiang, Z. L. Yin and Y. G. Xiao, *Chem. Eng. J.*, 2019, **367**, 249–259.
- Y. Z. Li, Y. Yu, L. Z. Wu and J. F. Zhi, *Appl. Surf. Sci.*, 2013, **273**, 135–143.
- L. Z. Wu, Y. Yu, X. Y. Han, Y. Zhang, Y. Zhang, Y. Z. Li and J. F. Zhi, *J. Mater. Chem. C*, 2014, **2**, 2266–2271.
- Y. Zhang, Y. Zhao, S. S. Cao, Z. L. Yin, L. Cheng and L. M. Wu, *ACS Appl. Mater. Interfaces*, 2017, **9**, 29982–29991.
- A. Dutschke, C. Diegelmann and P. Löbmann, *Chem. Mater.*, 2003, **15**, 3501–3506.
- L. Z. Wu, Y. Yu, L. Song and J. F. Zhi, *J. Colloid Interface Sci.*, 2015, **446**, 213–217.
- L. Z. Wu, Y. Yu and J. F. Zhi, *RSC Adv.*, 2015, **5**, 10159–10164.
- L. B. Yang, X. Jiang, W. D. Ruan, B. Zhao, W. Q. Xu and J. R. Lombardi, *J. Phys. Chem. C*, 2008, **112**, 20095–20098.
- M. Liu, L. Y. Piao, L. Zhao, S. T. Ju, Z. J. Yan, T. He, C. L. Zhou and W. J. Wang, *Chem. Commun.*, 2010, **46**, 1664–1666.
- L. C. Liu, X. R. Gu, Z. Y. Ji, W. X. Zou, C. J. Tang, F. Gao and L. Dong, *J. Phys. Chem. C*, 2013, **117**, 18578–18587.
- D. W. Li, L. J. Pan, S. Li, K. Liu, S. F. Wu and W. Peng, *J. Phys. Chem. C*, 2013, **117**, 6861–6871.
- K. Tanaka, K. Harada and S. Murata, *Sol. Energy*, 1985, **36**, 159–161.
- Z. Y. Wang, L. Zhou and X. W. Lou, *Adv. Mater.*, 2012, **24**, 1903–1911.
- P. A. Gross, S. N. Pronkin, T. Cottineau, N. Keller, V. Keller and E. R. Savinova, *Catal. Today*, 2012, **189**, 93–100.
- A. Takai and P. V. Kamat, *ACS Nano*, 2011, **5**, 7369–7376.

